A STUDY OF HULL FORM IMPROVEMENT FOR A FISHING TRAWLER

N. Xie[1], **I. Paton**[2] and **D. Vassalos**[1]

[1]Department of Naval Architecture and Marine Engineering, University of Strathclyde, 100 Montrose Street, Glasgow G4 0LZ, UK, d.vassalos@na-me.ac.uk
[2]S. C. McAllister & Co. Ltd

ABSTRACT

A study of hull form improvement for a trawler from resistance point of view has been carried out numerically. Both resistances in calm water and added resistance in waves are considered. Wave making resistance in calm water is calculated by a Rankine source distribution method. Added resistance in waves is predicted by the radiated energy method where ship motions are calculated by a strip theory. Based on the base hull, the longitudinal position of the centre of gravity of the vessel and a parameter to modify the hull form in the forebody are used to establish a response surface for the total resistance. An improved hull form and loading condition is found from the response surface in the parametric space, and a resistance reduction of 4.7 percent is achieved. Detailed numerical method for the prediction is presented.

Keywords: Ship resistance, Energy saving, Hull form, Resistance reduction, Added resistance in waves.

NOMENCLATURE

$\mathbf{a}$	Regression coefficient
(a,b,c)	Difference coefficients
$\mathbf{A,B,C}$	Matrix of equations for the source strength and vessel motions
b_{33}	Sectional heave damping coefficient
C_f	Coefficient of frictional resistance
f	Function
$\mathbf{F}$	Wave exciting force/moment vector
F_z	Vertical force
g	Acceleration due to gravity
$\mathbf{G}$	Vector of right hand side of the source equation
H_s	Significant wave height
k	Scale ratio
L_x, L_y	Directional cosine of the longitudinal curvature axis on the free surface
M_y	Trim moment
$\mathbf{n}$	Normal vector on a surface
p	Pressure
$\mathbf{P,Q}$	Matrix of the source strength equations
r	Distance between source and field points
R	Total resistance
R_f	Frictional resistance
Rn	Reynolds number
R_w	Wave making resistance
R_t	Total resistance in calm water
R_{aw}	Added resistance in regular wave
$\overline{R}_{aw}$	Mean added resistance in irregular wave
S_F	Free surface
S_H	Hull surface
S_w	Area of the wetted hull surface
S_ς	Wave spectrum
T	Draft
T_{01}	Average wave period
U	Ship speed
V_z	Vertical relative velocity at ship section
x, y, z	Coordinates
x_g	Longitudinal position of C.G.

Greek symbols

$(\alpha,\beta,\gamma,\delta)$	Difference coefficients
η	Free surface elevation
$\tilde{\eta}$	Free surface due to double body flow
ξ	Vessel motions
ς_a	Wave height
λ	Wavelength
ω	Wave frequency
ω_e	Encounter wave frequency
θ	Trim angle
Φ	Total velocity potential
ϕ	Velocity potential of double body flow
ϕ_∞	Velocity potential of incoming flow
φ	Velocity potential of disturbance flow
σ_0	Source strength of double body flow
σ_H	Source strength on hull of disturbance flow
σ_F	Source strength on free surface of disturbance flow
$\Im(\cdot)$	Function for free surface boundary condition

1. INTRODUCTION

The energy efficiency of a ship is always a concern in the shipbuilding industry due to rising fuel price and the international regulations on emissions. Among other factors, the EEDI (Energy Efficiency Design Index) proposed by IMO (2009) is proportional to the effective power of a ship, which is a product of the resistance and ship speed. A hull with lower resistance is desirable for ship designers, owners and operators. This is done at different stages of the design, and different approaches are adopted, including use of database, existing information of similar vessels,

numerical calculation (potential panel codes and/or viscous RANSE simulations) and model tests. Panel codes based on potential flow theory are widely used in the design offices nowadays, especially at the initial design stage, where various variants are to be evaluated. This is mainly due to the fact that the code is more efficient to run. It has been suggested that the panel method based on potential theory is capable of ranking relative merit of the design variants, especially when modifications are made to the forebody part of a hull. Goren et al (2004) have carried out a study for the forebody optimisation of a fishing vessel. The offset coordinates are used as the design variables and Michell's thin ship theory is used to predict the wave making resistance. The use of hull offset ordinates as the design variables may be prohibitively expensive when other solvers (such as a panel code) are adopted. There will also be issues for the fairness of the generated hull surface. Harries and Abt (1999) and Heimann and Harries (2003) presented a formal hydrodynamic optimization of a fast monohull on the basis of parametric hull design. The parametric approach consists of three steps: firstly, parametric design of a suitable set of longitudinal basic (primary) curves such as longitudinal sectional area curve and design waterline; secondly, parametric modelling of a sufficient number of design sections derived from the basic curves such as curve of tangent angles at either end and vertical moments of sectional area; and finally generation of a small set of surfaces interpolating the design sections. These parameters are higher level of descriptors of the hull geometry, and number of the design variables is reduced dramatically. SHIPFLOW code (Janson and Larsson, 1996) is adopted for the flow analysis. An example for optimization of the wave making characteristics of a ferry is provided. As mentioned by the authors, this hull geometry modelling tool still need modifications to handle more complicated shape such as bulbous bow. Grigoropoulos (2004) carried out a study of hull form optimization for hydrodynamic performance when both motion in waves and calm water resistance are considered.

In this paper, an investigation of hull form improvement with the objective of saving fuel (lower resistance) for a fishing trawler is carried out. Resistance of a trawler in calm water and added resistance in waves are addressed. The hull form is modified locally at the forebody area. Change of longitudinal position of the centre of gravity of the vessel is also considered. A response surface is established for the total resistance of the vessel. A Rankine source panel method is used for the wave-making resistance prediction and the added resistance in waves is predicted by the radiated energy method and a strip theory. A detailed description of the method and the numerical tests of the resistance code are presented. The method for wave making resistance prediction is similar to that of Dawson's (Dawson, 1977), but the treatment of the free surface boundary condition is different. In Dawson's original approach, the free surface boundary condition is discretised along stream lines of the double body flow, thus no lateral derivates are required. Dawson's method has been very successful and it is still used today. However, there is still margin for improvements. For example, at the bow and stern region where the stream lines are always coarse due to the stagnation, however, in order to resolve the flow field correctly, a fine grid is needed in these areas. Therefore, a general grid distribution is preferred (Jensen, 1990, Nakos and Sclavounos, 1994, Raven, 1996). In the prediction of the calm water resistance, the steady state running attitude of the vessel (sinkage and trim) is iteratively calculated by searching the vessel's dynamically balanced condition, where the wetted hull surface will change. The motion calculations in waves should also take into account the effect of the sinkage and trim. In this study, based on the base (parent) hull, a small number of variants have been designed and their resistance, wave pattern, pressure distribution and added resistance in waves are predicted. The total resistance of the vessel is fitted with a response surface. Thus the merit of each design can be assessed and an optimal design in this local design space can be found. The present approach is expected, hopefully, to be useful for the trawler designers.

2. PREDICTION OF RESISTANCE IN CALM WATER

2.1 MATHEMATICAL FORMULATIONS

A right handed coordinate system $o-xyz$ is set up with xoy plane on the undisturbed free surface, oz-axis is positive upwards, ox-axis pointing to the bow (Figure 1). We will discuss our problem within potential flow theory, which implies that the fluid is ideal and incompressible and the flow is irrotational. The vessel is advancing with forward speed U. A velocity potential exists, and it satisfies Laplace equation in the fluid domain:

$$\frac{\partial^2\Phi}{\partial x^2}+\frac{\partial^2\Phi}{\partial y^2}+\frac{\partial^2\Phi}{\partial z^2}=0 \qquad (1)$$

On the free surface, the dynamic boundary condition and the kinematic boundary condition should be satisfied:

$$\frac{1}{2}\nabla\Phi\cdot\nabla\Phi+gz-\frac{1}{2}U^2=0 \qquad \text{on } z=\eta(x,y) \qquad (2)$$

$$\nabla\Phi\cdot\nabla\eta=\frac{\partial\Phi}{\partial z} \qquad \text{on } z=\eta(x,y) \qquad (3)$$

On the hull surface:

$$\frac{\partial\Phi}{\partial n}=0 \qquad \text{on } S_H \qquad (4)$$

In addition, a far field radiation condition should be satisfied.

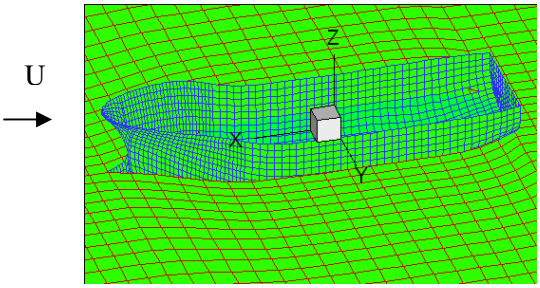

Figure 1: The coordinate system

The boundary value problem for the velocity potential formulated above is nonlinear due to the fact that the free surface boundary conditions themselves are nonlinear and they should be satisfied at an unknown free surface boundary. Substituting (2) into (3), one obtains

$$g\frac{\partial \Phi}{\partial z}+\frac{1}{2}\nabla\Phi\cdot\nabla(\nabla\Phi\cdot\nabla\Phi)=0 \qquad \text{on } z=\eta(x,y) \quad (5)$$

In the present study, this nonlinear free surface boundary condition is to be linearised. It is assumed that the velocity potential, $\Phi(x,y,z)$, consists of velocity potentials of the double body flow, $\phi(x,y,z)$, and the free surface disturbance flow, $\varphi(x,y,z)$:

$$\Phi(x,y,z)=\phi(x,y,z)+\varphi(x,y,z) \quad (6)$$

It is further assumed that the disturbance velocity potential, φ, is much smaller than that of the double body flow, ϕ. Thus, the free surface boundary condition (5) can be linearised. There are many ways to linearise the free surface boundary condition. One well known form is the Kelvin free surface condition in which the velocity potential is expanded about the undisturbed free surface with velocity potential of the free stream flow. In this study, the free surface boundary condition (5) is firstly expanded about the free surface of double body flow, $z=\tilde{\eta}$:

$$\Im(x,y,\eta)=\Im(x,y,\tilde{\eta})+\frac{\partial\Im(x,y,\tilde{\eta})}{\partial z}(\eta-\tilde{\eta})+\ldots \quad (7)$$

where the free surface elevation of the double body flow is

$$\tilde{\eta}(x,y)=\frac{1}{2g}\left(U^2-\nabla\phi\cdot\nabla\phi\right) \quad (8)$$

and

$$\Im(x,y,\eta)=g\frac{\partial\Phi}{\partial z}+\frac{1}{2}\nabla\Phi\cdot\nabla(\nabla\Phi\cdot\nabla\Phi) \quad (9)$$

Equation (7) is further expanded at the undisturbed free surface $z=0$ and the linearised free surface boundary condition about the disturbance flow potential, φ, becomes (Nakos et al, 1994, Xie et al, 2007)

$$\nabla\phi\cdot\nabla(\nabla\phi\cdot\nabla\varphi)+\frac{1}{2}\nabla\varphi\cdot\nabla(\nabla\phi\cdot\nabla\phi)+g\varphi_z-\phi_{zz}\nabla\phi\cdot\nabla\varphi$$

$$=-\frac{1}{2}\nabla\phi\cdot\nabla(\nabla\phi\cdot\nabla\phi)-\frac{1}{2}\phi_{zz}\left(U^2-\nabla\phi\cdot\nabla\phi\right) \qquad z=0 \quad (10)$$

The double body flow consists of the free stream incoming flow and a disturbance flow

$$\phi=\phi_\infty+\phi_H \quad (11)$$

where velocity potential of the incoming flow is

$$\phi_\infty=-Ux \quad (12)$$

The velocity potential for the double body disturbance flow satisfies the body boundary condition:

$$\frac{\partial\phi_H}{\partial n}=Un_1 \qquad \text{on } S_H \quad (13)$$

The velocity potentials are solved by a Rankine source distribution method. For the double body flow, Rankine sources are distributed on the wetted hull surface and its mirror about the undisturbed free surface ($z=0$):

$$\phi_H=\iint_{S_H+\hat{S}_H}\frac{\sigma_0}{r}ds \quad (14)$$

For the calculation of the velocity potential of the free surface disturbance flow, Rankine sources are distributed on the under water hull surface and the undisturbed free surface:

$$\varphi=\varphi_H+\varphi_F \quad (15)$$

where

$$\varphi_H=\iint_{S_H}\frac{\sigma_H}{r}ds \quad (16)$$

$$\varphi_F=\iint_{S_F}\frac{\sigma_F}{r}ds \quad (17)$$

where S_F is the free surface.

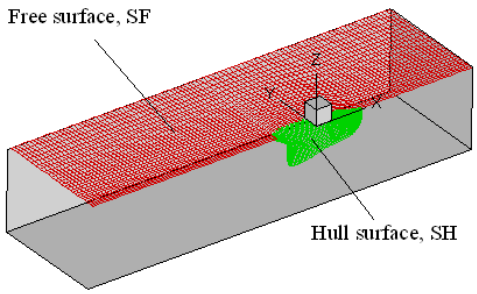

Figure 2: Boundaries of the flow field

2.2 NUMERICAL METHOD FOR THE RESISTANCE PROBLEM

The hull surface (S_H) and the free surface (S_F) are discretised into a number of quadrilateral elements, Figure 2. The source strength on each of the element is assumed as constant, and the Hess and Smith method (Hess and Smith, 1964) is used to solve for the unknown source strength. For the double body flow, with the hull surface boundary condition (13), the equations for the unknown source strength are

$$\sum_{j=1}^{NH} A_{i,j}\sigma_{0,j} = Un_{1,i} \qquad i = 1,2,...,NH \qquad (18)$$

where $A_{i,j}$ is the influence coefficient, NH is total number of elements for the hull surface. Solution of (18) will be the source strength of the double body flow.

For the disturbance flow, the following is obtained from the hull body boundary condition

$$\frac{\partial \varphi_H}{\partial n} + \frac{\partial \varphi_F}{\partial n} = 0 \qquad \text{on } S_H \qquad (19)$$

The discretised form of (19) is

$$\sum_{j=1}^{NH} B_{i,j}\sigma_{H,j} + \sum_{j=1}^{NF} C_{i,j}\sigma_{F,j} = 0 \qquad i = 1,2,...,NH \qquad (20)$$

The discretisation of the free surface boundary condition is more complex. Dawson had suggested an approach to discretise the free surface boundary condition along the stream lines of the double body flow to simplify the numerical calculation. In his method, only the derivates along a stream line are needed and no lateral derivates will be involved. However, this approach will result in a coarse grid distribution on the bow and stern region of the free surface where the flow changes rapidly. In the present study, a more general grid on the free surface is adopted, as it is presented in Figures 2 and 6. The free surface is discretised by a series of longitudinal ($y = y(x)$) and transverse ($x = \text{constant}$) lines, which are non-orthogonal. The following relations exist for the partial derivates on the free surface:

$$\begin{cases} f_x = \dfrac{1}{L_x} f_L - \dfrac{L_y}{L_x} f_T \\ f_y = f_T \end{cases} \qquad (21)$$

where f is a field function (e.g., velocity components), (L_x, L_y) are the directional cosines of the longitudinal curvature axis, $\vec{L}$. In order to discretise the free surface boundary condition (10), the longitudinal derivates are calculated by the 4-point upwind difference scheme, while the lateral derivates are calculated by a 3-point central difference scheme (Figure 3).

$$\begin{cases} (f_L)_{i,j} = \alpha_{i,j} f_{i,j} + \beta_{i,j} f_{i-1,j} + \gamma_{i,j} f_{i-2,j} + \delta_{i,j} f_{i-3,j} \\ (f_T)_{i,j} = a_{i,j} f_{i,j-1} + b_{i,j} f_{i,j} + c_{i,j} f_{i,j+1} \end{cases} \qquad (22)$$

where $\alpha_{i,j}, \beta_{i,j}, \gamma_{i,j}, \delta_{i,j}, a_{i,j}, b_{i,j}, c_{i,j}$ are the difference coefficients (Dawson, 1977, Bertram, 2002).

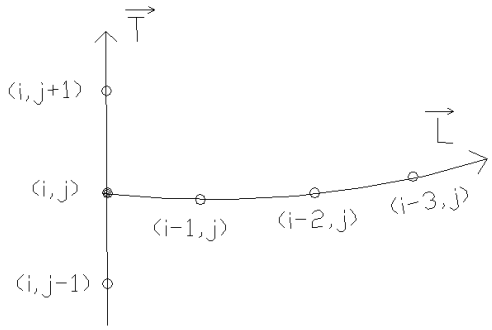

Figure 3: Numerical difference schemes on the free surface

For each panel on the free surface, one equation for the unknown source strength is obtained:

$$\sum_{j=1}^{NH} P_{i,j}\sigma_{H,j} + \sum_{j=1}^{NF} Q_{i,j}\sigma_{F,j} = G_i \qquad i = 1,2,...,NF \qquad (23)$$

Equations (20) and (23) are closed for the unknown source strength of velocity potential for the disturbance flow on hull and the free surface. These equations are solved by Gaussian elimination method.

Once the velocity potentials have been obtained, the pressure distribution in the fluid domain can be calculated by

$$p(x,y,z) = -\rho g z + \frac{1}{2}\rho(U^2 - \nabla\Phi \cdot \nabla\Phi) \qquad (24)$$

The wave making resistance is

$$R_w = -\iint_{S_H} p(x,y,z) n_1 ds \qquad (25)$$

The hydrodynamic vertical force and trim moment are

$$\begin{cases} F_z = \iint_{S_H} p(x,y,z) n_3 ds \\ M_y = \iint_{S_H} p(x,y,z)(z n_1 - x n_3) ds \end{cases} \qquad (26)$$

When a ship is freely running on the calm water surface, the total vertical force and trim moment should be balanced by weight of the ship (neglecting effects of other forces, such as components of propeller thrust, wind force etc):

$$\begin{cases} F_z(T,\theta) - mg = 0 \\ M_y(T,\theta) + mgx_g = 0 \end{cases} \qquad (27)$$

Therefore, for a ship with a given displacement and position of centre of gravity, the dynamically

balanced condition can be found by solving equation (27). In this study, these nonlinear equations are solved with Newton-Raphson method. The balanced position is searched along the gradient guided direction. The numerical iteration stops until a pre-set precision is achieved. The total resistance in calm water consists of frictional resistance and wave making resistance:

$$R_t = R_f + R_w \tag{28}$$

The frictional resistance of the vessel is calculated by ITTC57 formula.

$$R_f = C_f \cdot \frac{1}{2}\rho U^2 S_w \tag{29}$$

where S_w is area of the wetted hull surface, and the non-dimensional frictional resistance coefficient is

$$C_f = \frac{0.075}{(\log Rn - 2)^2} \tag{30}$$

where Rn is the Reynolds number based on ship length.

2.3 NUMERICAL TESTS FOR THE RESISTANCE CODE

Numerical calculations have been carried out for a fishing vessel, main particulars of which are shown in Table 1. Figure 4 shows body plan of the vessel. Both depart port and depart ground loading conditions are considered (Xie, 2010), only results of depart port loading condition are provided here. The contents of the numerical testing include size of the free surface boundary, schemes (aspect rations and expanding ratios for the grid) for discretising the free surface and the hull surface and treatment of the transom stern. The predicted results are compared with a model test measurement (Promara, 2008). For each vessel speed, the calculation starts with the floating condition in calm water (initial sinkage and trim), the hull surface and the free surface are discretised into panels and the flow field is solved by the potential code, yielding the pressure distribution over the wetted hull surface. With the unbalanced vertical force and trim moment, the vessel's attitude is adjusted. The new wetted hull surface and the free surface are re-panelised and the flow solver is called again. The iteration stops until a pre-set accuracy is met or a maximum iteration is reached. Figure 5 shows the panelised under water hull surface. Figure 6 shows the mesh on the free surface. Figures 7 and 8 show comparison of the results predicted by the present method and the model test measurement. The agreement is fairly satisfactory. The vessel hull surface is divided into 2550 panels while the free surface is divided into 4384 panels. The up stream boundary of the free surface is located at $1.5L$ from bow, and the down stream boundary is $3.5L$ from the stern. For sideways, the outer boundary is located at $y = 1.4L$, where L is the vessel length. Figure 9 shows a sample of the pressure distribution on the hull surface. The pressure distribution looks reasonable, high pressure regions are observed on the bow region of the hull. Figure 10 is an example of predicted wave pattern for the vessel at speed of 11 knots, where the Kelvin wave patterns are clearly observed. Wave peaks can be spotted on the bow and stern regions while a trough is located on the forward shoulder where high flow velocity and low pressure occur.

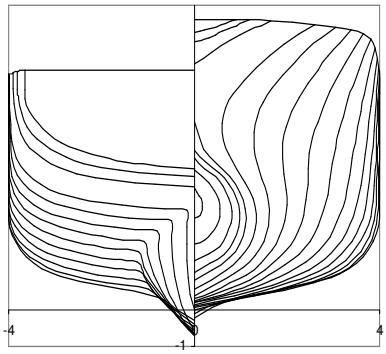

Figure 4: Body plan of the fishing vessel

Table 1: Main particulars of the fishing vessel

Overall length	$L_{OA}\ (m)$	27.9
width	$B\ (m)$	8.0
displacement	$\Delta\ (t)$	328.7
Centre of gravity	$x_g\ (m)$	-0.056
Mean draft	$T_0\ (m)$	3.88
Initial trim	$\theta_0\ (^0)$	-1.32

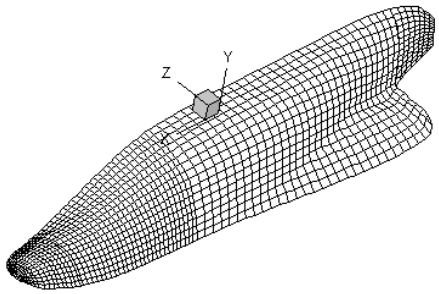

Figure 5: Panel grid on hull surface

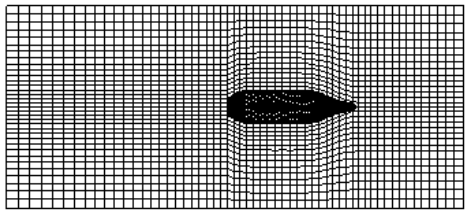

Figure 6: Grid on the free surface

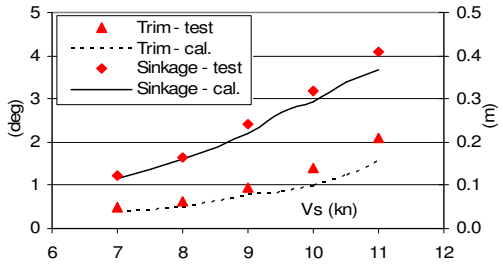

Figure 7: Comparison of sinkage and trim for a fishing vessel

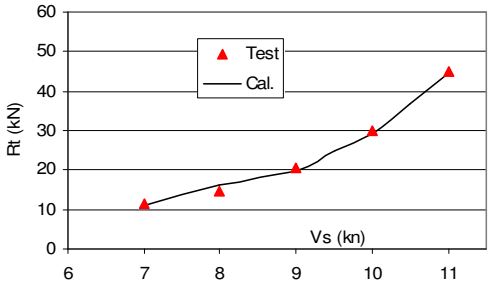

Figure 8: Comparison of resistance for a fishing vessel

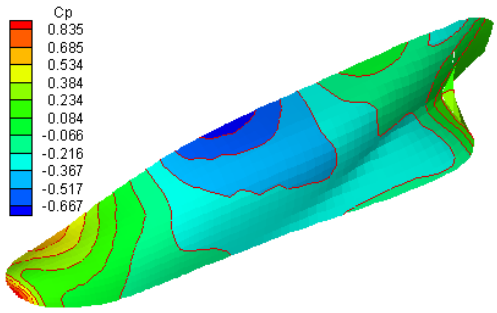

Figure 9: Pressure distribution of the vessel at U=9 knots

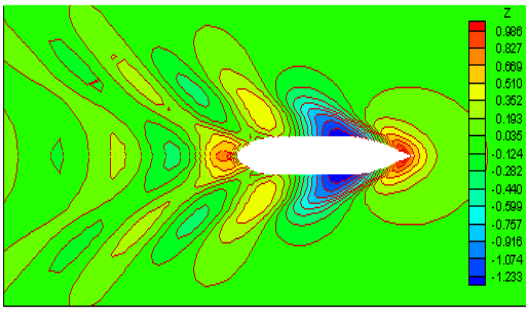

Figure 10: wave pattern of the fishing vessel at U=11 knots

3. PREDICTION OF THE ADDED RESISTANCE IN WAVES

The equations of motions of the vessel in regular wave can be written as

$$[\mathbf{M}+\mathbf{A}][\ddot{\xi}]+[\mathbf{B}][\dot{\xi}]+[\mathbf{C}][\xi]=[\mathbf{F}] \tag{31}$$

where $[\mathbf{M}]$ is mass matrix of the vessel, $[\mathbf{A}],[\mathbf{B}]$ and $[\mathbf{C}]$ are the matrices of added mass , damping coefficient and restoring force, respectively, $[\mathbf{F}]$ is the wave exciting force/moment vector. The hydrodynamic coefficients and wave excitation force are calculated by a strip theory (Salvensen et al., 1970, Xie et al., 2005). The 2D added mass and damping coefficients are predicted by the Frank close-fit method. The added resistance in wave is predicted by the radiated energy method (Gerritsma and Beukelman, 1972, Arribas, 2007):

$$R_{aw}=\frac{\pi}{\omega_e\lambda}\iint_L b_{33}(x)V_z^2(x)dx \tag{32}$$

where ω_e is encounter frequency, λ is length of the incident wave, $b_{33}(x)$ is the sectional heave damping coefficient, V_z is the local vertical relative velocity for the section. The mean added resistance in irregular waves is

$$\bar{R}_{aw}=2\int_0^\infty S_\varsigma(\omega_e)\frac{R_{aw}}{\varsigma_a^2}d\omega_e \tag{33}$$

where S_ς is wave spectrum, ς_a is wave amplitude of the regular incident wave. In this study, the ITTC standard wave spectrum is used

$$S_\varsigma(\omega)=A\omega^{-5}\exp\{-B/\omega^4\} \tag{34}$$

where $A=173.18H_s^2/T_{01}^4$ and $B=692.73/T_{01}^4$ with H_s significant wave height (m) and T_{01} average wave period (s).

4. A HULL FORM IMPROVEMENT STUDY

To demonstrate the applicability of the code in the improvement of the hull form design from the resistance point of view, a case study for a fishing vessel has been carried out. An existing hull of fishing trawler is selected as the base (parent) hull. The main particulars of the vessel are shown in Section 2. During this study, the forebody part of the hull is modified by a distortion method (Schneekluth and Bertram, 1998). The longitudinal coordinates of the offsets are scaled with a ratio, while the vertical and lateral coordinates are kept unchanged. The distortion starts from station number 16. Another factor to be studied is the initial loading condition, i.e., the longitudinal position of the centre of gravity of the vessel. The vessel speed is selected as 10 knots, and Froude number $Fn=0.335$. During the process, the displacement of the vessel is kept constant. For a series of longitudinal position of C.G., x_g, and the scale factor, k, the total resistance is predicted by the resistance and seakeeping codes. The output of the calm water steady flow calculation will be the wave-making resistance and the sinkage and trim of the vessel at the dynamically balanced condition. The total resistance in calm water will be the sum of the wave-making resistance and the frictional resistance which is calculated by ITTC57 formula.

With the sinkage and trim for a particular combination of x_g and k, the wetted hull surface is discretised for the seakeeping calculation and the mean added resistance in irregular wave is then predicted. For the present calculation, the wave parameters are selected as: significant wave height $H_s = 1.5m$ and average wave period $T_{01} = 6.5\sec.$ Only the added resistance in head waves is considered here. The total resistance is

$$R = R_t + \bar{R}_{aw} = f(x_g, k) \qquad (35)$$

The total resistance in (35) is expressed as surface given by a cubic polynomial:

$$R = \sum_{i=0}^{3}\sum_{j=0}^{3} a_{i,j} x_g^i k^j \qquad i + j \le 3 \qquad (36)$$

The response surface for the resistance is shown in Figure 11.

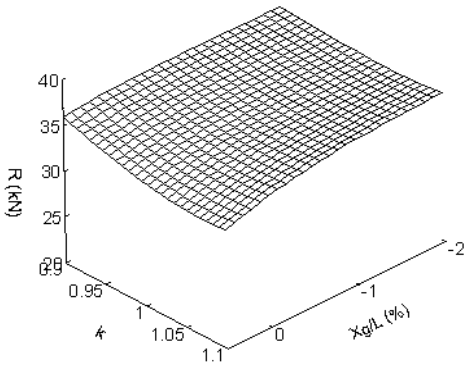

Figure 11: Response surface of the total resistance for a trawler at 10 knots

The regression coefficients in (36) are determined by the least square approach. The obtained regression coefficients are shown in Table 2. With the regression formula in (36), it is possible to find a hull form with k and longitudinal position of C.G., whose resistance is minimum in this local design space. In this case, $x_g = 0.5\%L_{PP}, k = 1.07$, the total resistance reduction is 4.7%. That is, by lengthening the fore body and moving the centre of gravity forward will result in reduction of the total resistance. Figure 12 shows a comparison of the wave profiles along the waterline for the base hull and the optimal hull. A slight decrease of the wave height in the bow region is observed. This reveals the wave making resistance reduction due to the changes of shape of bow and C.G. However, due to the relatively small parametric space, the difference is not so significant. Figure 13 and 14 shows the wave patterns for the original hull and the optimal hull, respectively.

The present method can be extended to the cases where more hull design parameters are included. More wide ranged optimization is possible if the parametric representation of the hull surface is available. From practical point of view, statistical wave data should be used for the sea area where the trawler is operating. Moreover, the trawler will have other operational loading conditions as well. Therefore, when considering the life time energy saving, all the scenarios should be taken into account.

Table 2: The regression coefficients ($a_{i,j}$)

$i \setminus j$	0	1	2	3
0	-99.562	517.88	-621.73	237.88
1	28.405	-51.492	21.445	—
2	1.143	-1.924	—	—
3	-0.154	—	—	—

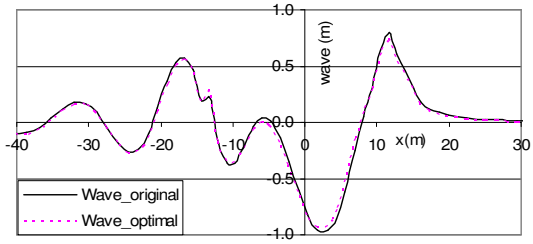

Figure 12: Comparison of wave profile along the hull

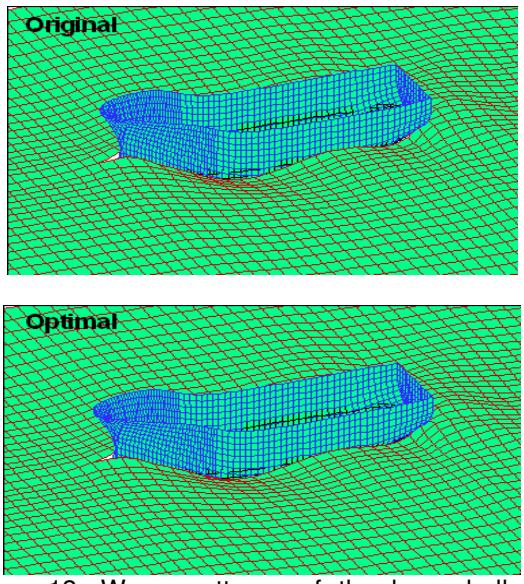

Figure 13: Wave patterns of the base hull and optimal hull, $U = 10$ knots

It should be pointed out that, any hull improvement built on numerical flow analysis can only be as good as the computational model employed. The neglect of certain flow phenomena might overestimate the benefit gained by the form variation. For example, viscous effects which alter the flow – particularly in the stern region – might decrease the advantageous interactions of waves generated along the hull although fast round-bilge mono-hulls with flow clearing at the transom usually are not prone to suffer from thick boundary layers. In addition, spray effects are not accounted in this

study either. Therefore, the full advantage predicted by the proposed method should followed by experimental validation studies in order to prove the validity of the hydrodynamic optimization based on potential flow calculations. Nevertheless, as more efficient simulation methods become available for optimization (due to the need for fast computations), the accuracy of studying the causes and effects between the geometric variations and the changes that they evoke in the flow field will further increase.

5. CONCLUSIONS

A method for improving the hull form design from a resistance point of view is presented. The resistance of a ship in calm water and added resistance in waves are treated. A detailed description of the resistance prediction is outlined. The potential panel code for the resistance prediction is verified with a model test measurement for a fishing trawler and a good agreement has been achieved. An example of hull form improvement is demonstrated for a trawler with modified forebody hull and loading conditions. A small number of design variants are established in order to form a response surface for the total resistance. Numerical results show that more than 4.7% gain for the resistance can be achieved in this relatively small design space. The method can be readily extended to include more design parameters for the hull geometry, this is a task that will be undertaken in the future. As far as the prediction of the added resistance in waves is concerned, the present study adopts a relatively simply model with a 2D strip theory. More advanced 3D method can be used to take into account the effect of the steady flow on the unsteady flow/forces and the 3D effect, which will be studied in the future as well.

ACKNOWLEDGEMENTS

The present study is partially funded by the EU project TARGET and the University of Strathclyde's StrathLINK founding scheme. Financial support from both sources is gratefully acknowledged by the authors.

REFERENCES

Arribas, F. P. (2007). 'Some methods to obtain the added resistance of a ship advancing in waves', Ocean Engineering, Vol. 34.

Bertram, V. (2002). 'Practical ship hydrodynamics', Butterworth-Heinemann.

Dawson, C. W. (1977). 'A Practical computer method for solving ship wave problems', Proceedings of 2nd International conference on Numerical Ship Hydrodynamics.

Gerritsma, J., Beukelman, W. (1972). 'Analysis of resistance increase in waves of a fast cargo ship', International Shipbuilding Progress, Vol. 19.

Goren, O., Danisman, D. B., Ozmen, G., Altar, M., Birmingham, R. W. (2004). 'Forebody optimization of a conventional fishing vessel operating at Fn=0.36', International Journal of Small Craft Technology.

Grigoropoulos, G. J. (2004). 'Hull form optimization for hydrodynamic performance', Journal of Ship Research, Vol. 41, No.4.

Harries, S., Abt, C. (1999). 'Formal hydrodynamic optimization of a fast mono-hull on the basis of parametric hull design', Proceedings of FAST'99, Seattle, USA.

Heimann, J., Harries, S. (2003). 'Optimization of the wave making characteristics of fast ferries', Applied Ocean Research, Vol. 25, No. 6.

Hess, J. L., Smith, A. M. O. (1964). 'Calculation of non-lifting potential flow about arbitrary three dimensional bodies', Journal of Ship Research, Vol. 8, No.2.

IMO, (2009), 'Interim guidelines on the method of calculation of the energy efficiency design index for new ships', MEPC.1/Circ.681.

Janson, C. E., Larsson, L. (1996). 'A Method for the optimization of ship hulls from a resistance point of view', 21st Symposium on Naval Hydrodynamics, Norway.

Jensen, G. (1990). 'Ship wave resistance computation', Proceedings of 5th International Conference on Numerical Ship Hydrodynamics.

Nakos, D. E., Sclavounos, P. D. (1994). 'Kelvin wakes and wave resistance of cruiser– and transom-stern ships', Journal of Ship Research, Vol. 38, No.1.

Promara. (2008). 'Model test to compare the fuel efficiency of two trawler designs', Report of Wolfson Unit, University of Southampton, Report No. 2101.

Raven, H. C. (1996). 'A Solution method for the nonlinear ship wave resistance problem', Ph. D thesis, Technique University of Delft.

Salvensen, N., Tuck, E., Faltinsen, O. (1970). 'Ship motions and sea loads', Transactions of SNAME, 78.

Schneckluth, H., Bertram, V. (1998). 'Ship design for efficiency and economy', Butterworth-Heinemann.

Xie, N. (2010). 'An Investigation of hull form improvement for a trawler', Report of NAME, University of Strathclyde.

Xie, N., Vassalos, D. (2005). 'A Study of the effect of steady flow on the unsteady motion of high speed craft', Proceedings of International Maritime Association of the Mediterranean Conference.

Xie, N., Vassalos, D., Sayer, P. (2007). 'The Effect of lift on the wave making resistance of multi-hull craft', International Shipbuilding Progress, Vol. 54, No. 2-3.